

IMPROVING SCALAR QUANTIZATION FOR CORRELATED PROCESSES USING ADAPTIVE CODEBOOKS ONLY AT THE RECEIVER

Sai Han and Tim Fingscheidt

Institute for Communications Technology, Technische Universität Braunschweig
Schleinitzstr. 22, 38106 Braunschweig, Germany
{s.han,t.fingscheidt}@tu-bs.de

ABSTRACT

Lloyd-Max quantization (LMQ) is a widely used scalar non-uniform quantization approach targeting for the minimum mean squared error (MMSE). Once designed, the quantizer codebook is fixed over time and does not take advantage of possible correlations in the input signals. Exploiting correlation in scalar quantization could be achieved by predictive quantization, however, for the price of a higher bit error sensitivity. In order to improve the Lloyd-Max quantizer performance for correlated processes without encoder-sided prediction, a novel scalar *decoding* approach utilizing the correlation of input signals is proposed in this paper. Based on previously received samples, the current sample can be predicted a priori. Thereafter, a quantization codebook adapted over time will be generated according to the prediction error probability density function. Compared to the standard LMQ, distinct improvement is achieved with our receiver in error-free and error-prone transmission conditions, both with hard-decision and soft-decision decoding.

Index Terms— Lloyd-Max quantization, correlated process, predictive quantization, probability density function, soft-decision decoding

1. INTRODUCTION

Quantization plays a key role in digital communications [1]. In [2] three categories of quantizers are identified: (1) Scalar quantization [3, 4], or vector quantization [5]; (2) quantizers with fixed-rate coding having the same codeword length for each quantization index [6, 7], or quantizers with variable-rate coding [8, 9]; (3) memoryless quantizers with the same quantization codebook over time [3, 4, 10], or quantizers with memory which means that the current quantization reconstruction levels are dependent on past samples [1, 11], with the memory referring to statistical properties of the source process.

When the input signal is correlated, memoryless scalar quantization is robust but inefficient, since it is designed in the same way for correlated as for uncorrelated processes. Therefore, the redundancy in terms of the correlation of source sig-

nals cannot be exploited. In contrast, utilizing the correlation in signals, predictive quantization [12, 13] and transform coding using an orthogonal transform matrix to decorrelate the source signals [14] are two major approaches of scalar quantization with memory.

Predictive quantization requires a quantizer inside a prediction loop at the transmitter and the same predictor is used to decode the signal at the receiver. The difference between the actual signal and its predictive estimate — the latter being based on previously reconstructed samples — is actually quantized. This is known from differential pulse code modulation (DPCM) [11], adaptive differential pulse code modulation (ADPCM) [15], and ADPCM-coded speech and audio [16]. However, due to error propagation, predictive coding is known to be sensitive to bit errors.

In order to achieve better performance in adverse transmission conditions, an additional error concealment is often desirable [17–19]. Hard-decision decoding and soft-decision decoding are two further alternative approaches in the receiver applicable to any of the above mentioned three major categories of quantizers. If soft information in the form of log-likelihood ratios (LLRs) containing channel reliability information is available, a soft-decision decoder could be used in the receiver [20–23], instead of error concealment which is typically based only on hard-decided bits.

In this paper, stemming from the idea of scalar quantization with memory, we present how to take advantage of the correlation in the source process, explicitly excluding vector quantization due to delay constraints. Different to predictive quantization which requires predictors both at the transmitter and the receiver side, we assume a non-predictive encoder and employ a predictor only at the receiver side. We utilize an instantaneous prediction error probability density function to compute a quantizer codebook with modified reconstruction levels in the receiver, adapted over time. Moreover, we compare the performance between standard LMQ and our new approach both with hard-decision and soft-decision decoding at the receiver. A particular advantage of our approach is its system-compatible use in decoders for robust non-predictive scalar quantizers in the encoder.

The paper is structured as follows: In Section 2, we de-

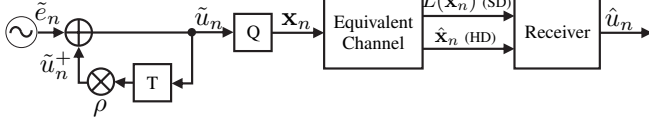


Fig. 1: Block diagram of the transmission system.

scribe the core of our new approach. Section 3 presents the receiver with hard-decision and soft-decision decoding. Simulation results are discussed in Section 4. Finally, some conclusions are drawn in Section 5.

2. IMPROVED LLOYD-MAX DECODING

2.1. Overview

The block diagram of the transmission system in our paper is depicted in Fig. 1. A first order autoregressive process (AR(1)) with the i.i.d. zero mean Gaussian innovation $\tilde{e} = (\tilde{e}_0, \tilde{e}_1, \dots, \tilde{e}_n, \dots)$ is used as input into the model for the (unquantized) correlated samples $\tilde{\mathbf{u}} = (\tilde{u}_0, \tilde{u}_1, \dots, \tilde{u}_n, \dots)$ satisfying $\tilde{u}_n = \tilde{e}_n + \rho \cdot \tilde{u}_{n-1}$, with $n \in \mathbb{N}^0$ being the time index and ρ being the correlation coefficient of the AR(1) process. After Lloyd-Max quantization (LMQ), each quantized sample u_n is represented by a quantizer bit combination in bipolar notation $\mathbf{x}_n = \{-1, +1\}^M$ corresponding to an M bit quantization index $i \in \mathcal{I} = \{0, 1, \dots, 2^M - 1\}$. Without loss of generality, the channel in this paper is described as an equivalent channel model comprising binary phase-shift keying (BPSK) modulation without any channel coding. For hard-decision decoding (HD), the received hard-decided bipolar bit combination $\hat{\mathbf{x}}_n = \{-1, 1\}^M$ is transformed to a received quantization index $\hat{i}_n \in \mathcal{I}$, which is further utilized at the receiver. In contrast, the log-likelihood ratios (LLRs) $L(\hat{\mathbf{x}}_n) = (L(\hat{x}_n(0)), L(\hat{x}_n(1)), \dots, L(\hat{x}_n(m)), \dots, L(\hat{x}_n(M-1))) \in \mathbb{R}^M$ of each received bit $\hat{x}_n(m) \in \{-1, +1\}$ are expected by a receiver employing soft-decision decoding (SD) [21], with bit index $m \in \{0, 1, \dots, M-1\}$.

2.2. New Adaptive LMQ Decoder Codebook

The core of our approach is to generate a new decoder quantization codebook adapted over time and depending on the past received samples. While decision levels are standard LMQ ones (as in the encoder), reconstruction levels are adaptively modified.

The well-known LMQ reconstruction levels for quantization index i read [1]

$$u^{(i)} = \frac{\int_{d_i}^{d_{i+1}} \tilde{u} \cdot p_{\tilde{U}}(\tilde{u}) d\tilde{u}}{\int_{d_i}^{d_{i+1}} p_{\tilde{U}}(\tilde{u}) d\tilde{u}}. \quad (1)$$

The reconstruction level $u^{(i)}$ is the centroid of the area of the sample probability density function (PDF) $p_{\tilde{U}}(\tilde{u})$ in the i -th

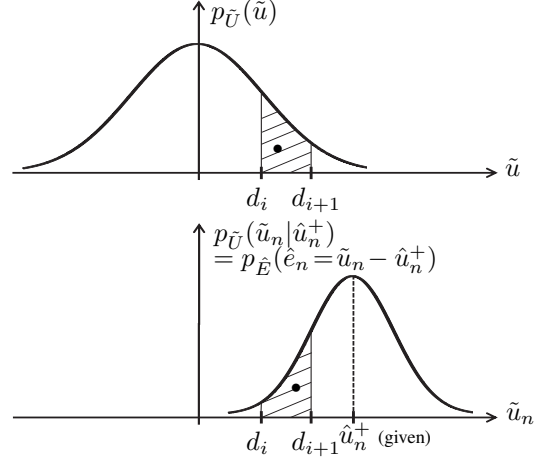


Fig. 2: Unquantized sample PDF and shifted PDF of the receiver-sided prediction error.

quantization interval (i. e., the area between decision levels d_i and d_{i+1}), which is shown as black dot in the upper plot of Fig. 2.

However, for correlated samples, after estimation of the previous sample \hat{u}_{n-1} in the receiver, a respective predicted sample \hat{u}_n^+ at current time index n can be obtained according to (in the AR(1) case)

$$\hat{u}_n^+ = \rho \cdot \hat{u}_{n-1}, \quad (2)$$

adopting the correlation coefficient ρ from the unquantized signal $\tilde{\mathbf{u}}$. Note that the predictor memory is initialized with zeros, meaning $\hat{u}_{n-1} = 0$ for $n \leq 0$.

If we are interested in $u^{(i)}$ for a fixed received $i = \hat{i}_n$ at time n , given the predicted sample \hat{u}_n^+ (representing the past received samples), (1) becomes

$$u_n^{(i)} = \frac{\int_{d_i}^{d_{i+1}} \tilde{u}_n \cdot p_{\tilde{U}}(\tilde{u}_n | \hat{u}_n^+) d\tilde{u}_n}{\int_{d_i}^{d_{i+1}} p_{\tilde{U}}(\tilde{u}_n | \hat{u}_n^+) d\tilde{u}_n}. \quad (3)$$

For the Gaussian AR(1) process from Fig. 1 we easily see that for a given $\hat{u}_n^+ = \rho \cdot \hat{u}_{n-1}$, the PDF of \tilde{u}_n results in $p_{\tilde{U}}(\tilde{u}_n | \hat{u}_n^+) = p_{\hat{E}}(\hat{e}_n = \tilde{u}_n - \hat{u}_n^+) = f(\tilde{u}_n)$, which is the transmitter-sided prediction error PDF $p_{\hat{E}}(\cdot)$ shifted by \hat{u}_n^+ . Applying this to the receiver and replacing \tilde{u}_n^+ by \hat{u}_n^+ as it is given by (2), we can write $p_{\tilde{U}}(\tilde{u}_n | \hat{u}_n^+) = p_{\hat{E}}(\hat{e}_n = \tilde{u}_n - \hat{u}_n^+) = f(\tilde{u}_n)$, with the shifted receiver-sided prediction error PDF $p_{\hat{E}}(\hat{e}_n = \tilde{u}_n - \hat{u}_n^+)$ being sketched in the lower graph of Fig. 2. Note that $p_{\hat{E}}(\cdot)$ in general has a lower variance than $p_{\tilde{U}}(\tilde{u})$. Also note that the shape of $p_{\hat{E}}(\cdot)$ in quantization interval $[d_i, d_{i+1}]$ is quite different from $p_{\tilde{U}}(\tilde{u})$. The optimal reconstruction values are then

$$u_n^{(i)} = \frac{\int_{d_i}^{d_{i+1}} \tilde{u}_n \cdot p_{\hat{E}}(\hat{e}_n = \tilde{u}_n - \hat{u}_n^+) d\tilde{u}_n}{\int_{d_i}^{d_{i+1}} p_{\hat{E}}(\hat{e}_n = \tilde{u}_n - \hat{u}_n^+) d\tilde{u}_n}, \quad (4)$$

while the decision levels d_i and d_{i+1} from the standard LMQ are kept according to the given received index $i = \hat{i}_n$.

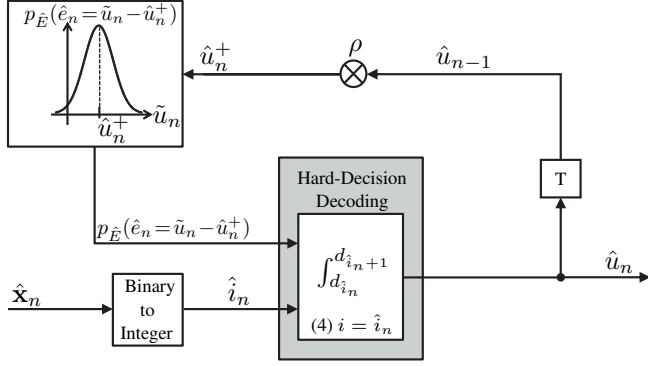


Fig. 3: Block diagram of the newly proposed receiver with hard-decision decoding (HD).

The shifted prediction error PDF as used in (4) is given by:

$$p_{\hat{E}}(\hat{e}_n = \tilde{u}_n - \hat{u}_n^+) = \frac{1}{\sqrt{2\pi}\sigma} \exp\left(-\frac{(\tilde{u}_n - \mu)^2}{2\sigma^2}\right), \quad (5)$$

with the mean $\mu = \hat{u}_n^+$, and variance σ^2 . Note that equation (4) can be easily solved numerically with the help of the error function.

Finally, the estimated sample \hat{u}_n is given by computing (4) for each time n using the received index \hat{i}_n (hard-decision decoding). For soft-decision decoding it must be done for all $i \in \mathcal{I}$, followed by further computations.

3. FURTHER DECODER OPTIONS

The receiver can either employ conventional hard-decision decoding (HD) or soft-decision decoding (SD). While SD is mostly applicable to mobile transmission, HD can always be employed, particularly in voice over IP (VoIP).

3.1. Using Hard Decisions

Fig. 3 shows the diagram of the new decoder employing conventional hard decisions. Note that the quantization index i in (4) is replaced by the received quantization index \hat{i}_n .

3.2. Using Soft Decisions

For the new decoder employing soft decisions as depicted in Fig. 4, a new LMQ codebook and *a posteriori* probabilities $P(\mathbf{x}_n^{(i)} | \hat{\mathbf{x}}_0^n)$ (APPs) of a probably transmitted bit combination $\mathbf{x}_n^{(i)}$ with respect to all the received bit combinations $\hat{\mathbf{x}}_0^n = (\hat{\mathbf{x}}_0, \hat{\mathbf{x}}_1, \dots, \hat{\mathbf{x}}_n)$ are needed for the sample estimation [21].

Assuming an additive white Gaussian noise (AWGN) channel, the log-likelihood ratios (LLRs) being input into the receiver with soft-decision decoding in Fig. 4, can be obtained by $L(\hat{x}_n(m)) = 4 \cdot \frac{E_b}{N_0} \cdot \tilde{x}_n(m)$, with $\tilde{x}_n(m)$ being the real-valued signal observed at the (noisy) transmission channel output satisfying $\hat{x}_n(m) = \text{sign}(L(\hat{x}_n(m))) = \text{sign}(\tilde{x}_n(m))$,

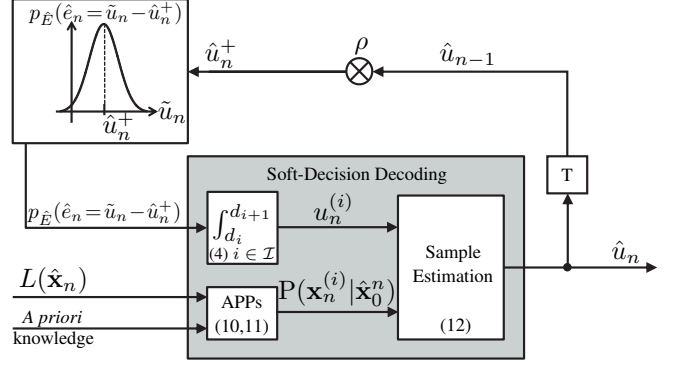


Fig. 4: Block diagram of the newly proposed receiver with soft-decision decoding (SD).

the signal energy per bit E_b , and N_0 being the noise power spectral density. Accordingly, a bit error probability is given by $\text{BER}_n(m) = \frac{1}{1 + \exp(|L(\hat{x}_n(m))|)}$. Thereafter, assuming a memoryless channel, the probabilities of the transition from a possibly transmitted bit combination $\mathbf{x}_n^{(i)}$ to a received bit combination $\hat{\mathbf{x}}_n$ (i. e., the transition probabilities) is formulated by

$$P(\hat{\mathbf{x}}_n | \mathbf{x}_n^{(i)}) = \prod_{m=0}^{M-1} P(\hat{x}_n(m) | x_n^{(i)}(m)), \quad (6)$$

with $x_n^{(i)}(m)$ being a possibly transmitted bit and the conditional bit probability

$$P(\hat{x}_n(m) | x_n^{(i)}(m)) = \begin{cases} 1 - \text{BER}_n(m), & \text{if } \hat{x}_n(m) = x_n^{(i)}(m), \\ \text{BER}_n(m), & \text{else.} \end{cases} \quad (7)$$

3.2.1. A Posteriori Probabilities (APPs)

Not only the transition probabilities, but also some *a priori* knowledge is employed to compute the *a posteriori* probabilities $P(\mathbf{x}_n^{(i)} | \hat{\mathbf{x}}_0^n)$. A large training database is required to be processed beforehand to derive the *a priori* knowledge. The quantized parameters could be regarded as the output of a zeroth-order Markov process leading to zeroth-order *a priori* knowledge $P(\mathbf{x}_n^{(i)})$ (AK0), or as a first-order Markov process resulting in first-order *a priori* knowledge $P(\mathbf{x}_n^{(i)} | \mathbf{x}_{n-1}^{(j)})$ (AK1). The occurrence frequency for different pairs of quantizer output symbols is counted and normalized to obtain the joint probability $P(\mathbf{x}_n^{(i)}, \mathbf{x}_{n-1}^{(j)})$, thereafter, the AK0 term is obtained from

$$P(\mathbf{x}_n^{(i)}) = \sum_{j \in \mathcal{I}} P(\mathbf{x}_n^{(i)}, \mathbf{x}_{n-1}^{(j)}). \quad (8)$$

According to the chain rule, the AK1 term is computed by

$$P(\mathbf{x}_n^{(i)} | \mathbf{x}_{n-1}^{(j)}) = \frac{P(\mathbf{x}_n^{(i)}, \mathbf{x}_{n-1}^{(j)})}{\sum_{k \in \mathcal{I}} P(\mathbf{x}_n^{(k)}, \mathbf{x}_{n-1}^{(j)})}. \quad (9)$$

Applying the AK0 or AK1 term, the *a posteriori* probabilities can be obtained either by [21]

$$P(\mathbf{x}_n^{(i)} | \hat{\mathbf{x}}_0^n) = \frac{1}{C_n} \cdot P(\hat{\mathbf{x}}_n | \mathbf{x}_n^{(i)}) \cdot P(\mathbf{x}_n^{(i)}), \quad (10)$$

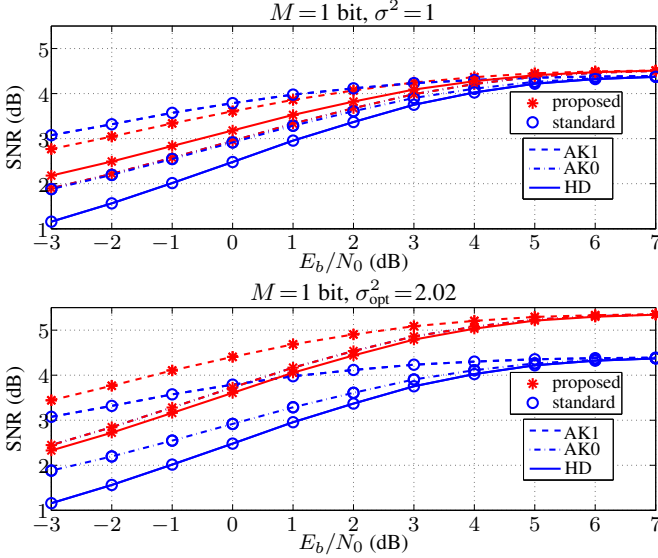


Fig. 5: Simulation results for $M = 1$ bit quantized Gaussian AR(1) samples with correlation coefficient $\rho = 0.9$.

or

$$P(\mathbf{x}_n^{(i)}|\hat{\mathbf{x}}_0^n) = \frac{1}{C_n} \cdot P(\hat{\mathbf{x}}_n|\mathbf{x}_n^{(i)}) \cdot \sum_{j \in \mathcal{I}} P(\mathbf{x}_n^{(i)}|\mathbf{x}_{n-1}^{(j)}) \cdot P(\mathbf{x}_{n-1}^{(j)}|\hat{\mathbf{x}}_0^{n-1}), \quad (11)$$

with C_n normalizing the sum over the APPs to one.

3.2.2. Sample Estimation

Using the APPs (10) or (11) and the new time-varying LMQ decoder codebook (4), the sample u_n at time index n can be reconstructed by minimum mean-square error (MMSE) estimation:

$$\hat{u}_n = \sum_{i \in \mathcal{I}} u_n^{(i)} \cdot P(\mathbf{x}_n^{(i)}|\hat{\mathbf{x}}_0^n). \quad (12)$$

4. SIMULATIONS

4.1. Simulation Setup

Lloyd-Max quantizers for 1 bit, 2 bit, and 3 bit per sample are employed in three separate simulations, respectively. In each simulation, a number of 10^6 zero mean unit variance Gaussian AR(1) samples with $\rho = 0.9$ is transmitted over different channel realizations for a given range of E_b/N_0 values. The bit mapping $u_n \rightarrow \mathbf{x}_n$ follows the natural binary code (NBC) [1]. A number of 10^8 quantized Gaussian AR(1) samples with correlation $\rho = 0.9$ is utilized to obtain the AK0 and AK1 *a priori* probability terms (8), (9). The performance is evaluated by means of the global signal-to-noise ratio (SNR) [21] with reference to the 10^6 yet unquantized samples $\tilde{\mathbf{u}}$.

4.2. Discussion

The simulation results of using the standard LMQ and our new approach are compared in Figs. 5 and 6, with HD denot-

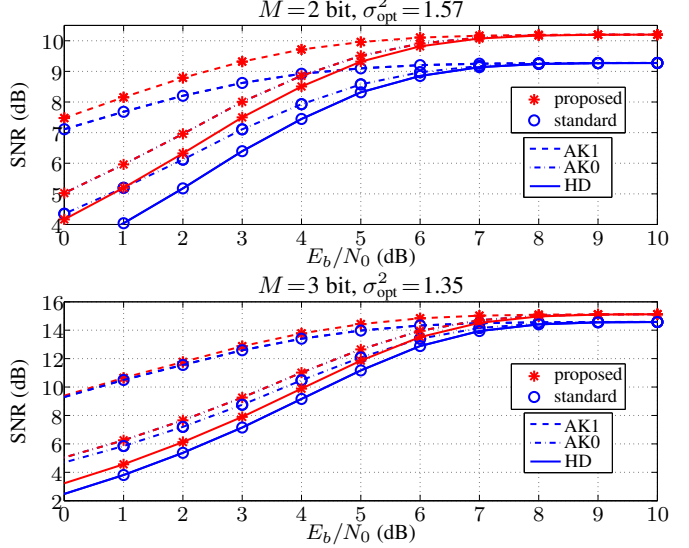


Fig. 6: Simulation results for $M = 2$ bit, $M = 3$ bit quantized Gaussian AR(1) samples with correlation coefficient $\rho = 0.9$.

LMQ	ρ					
	0	0.3	0.5	0.7	0.8	0.9
standard	9.30	9.30	9.30	9.30	9.30	9.30
new	9.30	9.35	9.45	9.67	9.86	10.20

Table 1: SNR (dB) of the standard LMQ and the new LMQ for an $M = 2$ bit quantized Gaussian AR(1) process with different correlation coefficients ρ in error-free transmission.

ing the use of hard decisions according to Fig. 3, AK0 and AK1 representing soft-decision decoding according to Fig. 4, with zeroth-order and first-order *a priori* knowledge, respectively. As shown in Fig. 5, we first performed experiments for $M = 1$ bit. It can be observed in the upper graph in Fig. 5 that the performance particularly of hard decision has been improved with the new approach. In fact, $\sigma^2 = 1$ in (5) is actually not an optimum value for equation (4). Clear further improvements can be obtained by searching for an optimal σ_{opt}^2 in error-free transmission. It can be seen in the lower graph of Fig. 5 that the SNR gain of our approach vs. standard LMQ *in error-free transmission conditions* can be increased from 0.1 dB ($\sigma^2 = 1$) to 1.0 dB ($\sigma_{\text{opt}}^2 = 2.02$)!

We also performed simulations with $M = 2$ bit and $M = 3$ bit using the respective optimized variances for the decoder codebook. The use of our new approach again leads to prominent improvements versus the standard LMQ, especially for the lower bit rate ($M = 2$ bit). Both HD and SD approaches take profit. Comparing the simulation results for $M = 1, 2, 3$ bit, we can state that the new approach takes particular profit from low bit rate scalar quantization.

The effect of the correlation has been further investigated by varying the correlation coefficients ρ for $M = 2$ bit with the respective optimized variances in error-free transmission conditions. Table 1 reveals increasing SNR gains for higher correlation coefficients. For uncorrelated processes ($\rho = 0$) we obtain $\hat{u}_n^+ = 0$, leading to the standard zero-mean PDF

$p_{\hat{E}}(\hat{e}_n = \tilde{u}_n - 0) \equiv p_{\tilde{U}}(\tilde{u}_n)$. In consequence, the SNR of using the standard LMQ and the new LMQ decoder in this case converge to be the same.

5. CONCLUSIONS

In this paper we present a new approach to improve the decoding performance of scalar Lloyd-Max quantizers (LMQs) for correlated samples. An adaptive new LMQ decoder codebook can be obtained by exploiting the signal PDF conditioned on a predicted sample. Simulations over an AWGN channel show that our novel approach exceeds the standard LMQ approach both in error-free and error-prone transmission conditions, especially for low bit rate scalar quantization of highly correlated processes, while being compatible with standard LMQ encoders.

REFERENCES

- [1] N.S. Jayant and P. Noll, *Digital Coding of Waveforms*, Prentice-Hall, Inc., Englewood Cliffs, New Jersey, 1984.
- [2] R.M. Gray and D.L. Neuhoff, "Quantization," *IEEE Trans. Inf. Theory*, vol. 44, no. 6, pp. 2325–2383, Oct. 1998.
- [3] S.P. Lloyd, "Least Squares Quantization in PCM," *IEEE Trans. Inf. Theory*, vol. 28, no. 2, pp. 129–136, Mar. 1982.
- [4] J. Max, "Quantizing for Minimum Distortion," *IRE Transactions on Information Theory*, vol. 6, no. 1, pp. 7–12, Mar. 1960.
- [5] Y. Linde, A. Buzo, and R.M. Gray, "An Algorithm for Vector Quantizer Design," *IEEE Trans. Commun.*, vol. 28, no. 1, pp. 84–95, Jan. 1980.
- [6] B.M. Oliver, J.R. Pierce, and C.E. Shannon, "The Philosophy of PCM," *Proceedings IRE*, vol. 36, no. 11, pp. 1324–1331, Nov. 1948.
- [7] D. Hui and D.L. Neuhoff, "Asymptotic Analysis of Optimal Fixed-Rate Uniform Scalar Quantization," *IEEE Trans. Inf. Theory*, vol. 47, no. 3, pp. 957–977, Mar. 2001.
- [8] T. Lookabaugh, E.A. Riskin, P.A. Chou, and R.M. Gray, "Variable Rate Vector Quantization for Speech, Image, and Video Compression," *IEEE Trans. Commun.*, vol. 41, no. 1, pp. 186–199, Jan. 1993.
- [9] S. Han and T. Fingscheidt, "Variable-Length Versus Fixed-Length Coding: On Tradeoffs for Soft-Decision Decoding," in *Proc. of ICASSP 2014*, Florence, Italy, May 2014.
- [10] W.B. Kleijn and R. Hagen, "On Memoryless Quantization in Speech Coding," *IEEE Signal Process. Lett.*, vol. 3, no. 8, pp. 228–230, Aug. 1996.
- [11] R. A. McDonald, "Signal-to-Noise and Idle Channel Performance of Differential Pulse Code Modulation Systems — Particular Applications to Voice Signals," *Bell System Technical Journal*, vol. 45, no. 7, pp. 1123–1151, Sept. 1966.
- [12] P. Elias, "Predictive Coding—I," *IRE Transactions on Information Theory*, vol. 1, no. 1, pp. 16–24, Mar. 1955.
- [13] D.S. Arnstein, "Quantization Error in Predictive Coders," *IEEE Trans. Commun.*, vol. 23, no. 4, pp. 423–429, Apr. 1975.
- [14] J. Huang and P.M. Schultheiss, "Block Quantization of Correlated Gaussian Random Variables," *IEEE Transactions on Communications Systems*, vol. 11, no. 3, pp. 289–296, Sept. 1963.
- [15] P. Cummiskey, N. S. Jayant, and J. L. Flanagan, "Adaptive Quantization in Differential PCM Coding of Speech," *Bell System Technical Journal*, vol. 52, no. 7, pp. 1105–1118, Sept. 1973.
- [16] "ITU-T Recommendation G.722, 7 kHz Audio-Coding Within 64 kbit/s," ITU, Nov. 1988.
- [17] "ITU-T Recommendation G.711 Appendix I, A High Quality Low-Complexity Algorithm for Packet Loss Concealment with G.711," ITU-T, Sept. 1999.
- [18] "ITU-T Recommendation G.722 Appendix III, A High-Quality Packet Loss Concealment Algorithm for G.722," ITU-T, Nov. 2006.
- [19] M. Serizawa and Y. Nozawa, "A Packet Loss Concealment Method Using Pitch Waveform Repetition and Internal State Update on the Decoded Speech for the Sub-Band ADPCM Wideband Speech Codec," in *Proc. of IEEE Workshop Speech Coding*, Tsukuba City, Japan, Oct. 2002, pp. 68–70.
- [20] V. Cuperman, F.-H. Liu, and P. Ho, "Robust Vector Quantization for Noisy Channels Using Soft Decision and Sequential Decoding," *Europ. Trans. Telecomm.*, vol. 5, no. 5, pp. 7–18, Sept. 1994.
- [21] T. Fingscheidt and P. Vary, "Softbit Speech Decoding: A New Approach to Error Concealment," *IEEE Trans. Speech, Audio Process.*, vol. 9, no. 3, pp. 240–251, Mar. 2001.
- [22] T. Fingscheidt, "Parameter Models and Estimators in Soft Decision Source Decoding," in *Advances in Digital Speech Transmission*, R. Martin, U. Heute, and C. Antweiler, Eds., pp. 281–310. John Wiley & Sons, Ltd, West Sussex, England, 2008.
- [23] S. Han, F. Pflug, and T. Fingscheidt, "Improved AMR Wideband Error Concealment for Mobile Communications," in *Proc. of EUSIPCO 2013*, Marrakech, Morocco, Sept. 2013.